Image findings of anti-neutrophil cytoplasmic antibody-associated vasculitis involving the skull base

S.Y. Yun [a,b], Y.J. Choi [a,*], S.R. Chung [a], C.H. Suh [a], S.C. Kim [a], J.H. Lee [a], J.H. Baek [a]

[a] Department of Radiology and Research Institute of Radiology, Asan Medical Center, University of Ulsan College of Medicine, Seoul, Republic of Korea
[b] Department of Radiology, Inje University Busan Paik Hospital, Busan, Republic of Korea

ARTICLE INFORMATION

AIM: To investigate computed tomography (CT) and magnetic resonance imaging (MRI) features of skull bases involving anti-neutrophil cytoplasmic antibody (ANCA)-associated vasculitides (AAV).

MATERIALS AND METHODS: A retrospective review was undertaken to identify an institutional historical cohort of 17 patients with confirmed AAV who underwent CT or MRI and had skull base involvement between 2002 and 2021. Two radiologists reviewed the extent and features of the lesions, bone changes, and other MRI findings.

RESULTS: A total of 17 patients (12 men; mean age $\pm$ standard deviation, 46.5 $\pm$ 17.1 years) were selected. AAV presented as infiltrative lesions with involvement at various sites. Most cases involved the paranasal sinuses (PNS; 88%, 15/17), nasopharynx (88%, 15/17), pterygopalatine fossa (82%, 14/17), and parapharyngeal space (82%, 14/17), frequently accompanied by mucosal irregularity of the PNS and nasopharynx (71%, 12/17). Central skull base and temporal bone involvement were seen in 53% (9/17) and 38% (6/16) of cases, respectively. On T1-weighted imaging (WI) and T2WI MRI, all lesions (15/15) showed predominant signal iso-intensity to grey matter.

CONCLUSIONS: Although radiological findings of AAV are non-specific and skull base involvement is less common, AAV may be considered if infiltrative lesions predominantly involving the PNS, nasopharynx, pterygopalatine fossa, and parapharyngeal space with combined bone changes of skull base are seen.

© 2023 Published by Elsevier Ltd on behalf of The Royal College of Radiologists.

* Guarantor and correspondent: Y. J. Choi, Department of Radiology and Research Institute of Radiology, Asan Medical Center, University of Ulsan College of Medicine, 88, Olympic-ro 43-Gil, Songpa-gu, Seoul, 05505, Republic of Korea. Tel.: +82 2 3010-4400; fax: +82 2 476-0090.
E-mail address: jehee23@gmail.com (Y.J. Choi).

Introduction

Anti-neutrophil cytoplasmic antibody (ANCA)-associated vasculitides (AAVs) are rare diseases characterised by necrotising vasculitis with few or no immune deposits, predominantly affecting small vessels.[1,2] AAVs are classified into three types: granulomatosis with polyangiitis (GPA, previously called Wegener's granulomatosis), microscopic polyangiitis (MPA), and eosinophilic GPA (EGPA).[1,3] GPA is predominantly associated with proteinase-3 (PR3)-ANCA, MPA is usually associated with myeloperoxidase (MPO)-ANCA, and EGPA is characterised by asthma, eosinophilia and, in many cases, vasculitis.[1] Probably due to improving survival and better case definition, the prevalence rates are increasing, with recent studies estimating a prevalence of 300–421 per million people.[4,5] All forms of AAV can present with manifestations relating to small vessel vasculitic lesions and dysfunction of any organ[6]; however, GPA shows more frequent head and neck region involvement, than MPA and EGPA.[1] In particular, the nasal cavity and the paranasal sinuses (PNS) are the most common sites of involvement in the head and neck region (85–100%) in GPA.[7,8]

The multiple manifestations of AAV make diagnosis challenging,[8] and the skull base is rarely involved in patients with GPA.[9–18] Several studies have reported imaging findings of head and neck involvement of GPA,[8,13,19–24] among them, a few review articles have briefly commented on the imaging finding of the skull in patients with GPA.[8,21] To date, there has been no original article reporting the computed tomography (CT) and magnetic resonance imaging (MRI) findings of AAV involving the skull base. Therefore, the purpose of the present study was to assess the CT and MRI findings of the patients with AAV involving the skull base.

MATERIALS and METHODS

Patients

The present study was approved by the local ethics committee and the institutional review board (IRB), and the requirement for informed consent was waived due to the retrospective nature of the study (IRB number: 2021-1734). The protocols and data reporting were performed in accordance with STROBE (Strengthening the Reporting of Observational Studies in Epidemiology) guidelines.[25,26]

The study population was obtained from a historical cohort of patients who were diagnosed with AAV at Asan Medical Center between May 2002 and July 2021. AAV was diagnosed in accordance with the 2012 international Chapel Hill Consensus Conference[2,27] and 2017 American College of Rheumatology/European League Against Rheumatism provisional classification criteria.[28] The inclusion criteria were[1]: patients who were diagnosed with AAV,[2] patient who underwent CT or MRI of the head and neck region, and[3] patients in whom the skull base involvement was evident on CT or MRI as determined by two neuroradiologists who were blinded to the original radiology report. A total of 17 patients were included in this study. The medical records of the included patients were reviewed thoroughly. Clinical data including age at the time of biopsy, sex, biopsy site, and ANCA phenotypes were collected. ANCA phenotypes were divided into MPO positive patients, PR3 positive patients, and not detected.

Image acquisition

All 17 patients underwent CT on one of several different multidetector CT systems with 16–128 channels (Siemens Medical Solutions, Erlangen, Germany; GE Healthcare, Milwaukee, WI, USA). MRI was performed in 15 patients: three patients were scanned with 1.5 T MRI (Magnetom Vision, Siemens) with a section thickness 2 or 3 mm, and the 12 remaining patients were scanned with 3 T MRI (Achieva, Philips Medical Systems, Best, The Netherlands; Ingenia, Philips Medical Systems, Best, The Netherlands). The MRI protocol contained the following sequences: axial T1-weighted imaging (WI), axial T2WI, coronal T1WI, coronal fat-suppressed T2WI, axial fat-suppressed contrast-enhanced T1WI, and coronal fat-suppressed contrast-enhanced T1WI, section thickness 3 mm without gap.

Image analysis

All CT or MRI studies were interpreted by two board-certified radiologists, with 6 and 14 years of clinical experience in head and neck imaging. The radiologists reviewed the imaging in consensus and rated the extent (involvement of PNS, parapharyngeal space, prevertebral space, orbit, pterygopalatine fossa, central skull base, temporal bone, cranial cavity, nasopharynx, masticator space), bone destruction, bone sclerosis, bone marrow signal change, presence of soft-tissue necrosis, mucosal irregularity, and the T1 and T2 characteristics of the lesion. The central skull base included the sphenoid, temporal bone anterior to the petrous ridge, multiple foramina and fissures (foramen ovale, foramen spinosum, foramen rotundum, foramen lacerum, superior orbital fissure, inferior orbital fissure, optic canal, carotid canal and vidian canal).[29,30] As the contiguous spread of granulomatous tissue from adjacent sites was considered as a mechanism of CNS involvement, involvement of the pituitary gland or dura adjacent to the central skull base was classified as cranial cavity involvement.[31] Bone destruction and sclerosis were determined by CT findings, and bone marrow signal changes were detected using T1WI from MRI. The presence of soft-tissue necrosis was defined as the non-enhancing soft-tissue portion in the lesion, which was determined using fat-suppressed contrast-enhanced T1WI from MRI. Mucosal irregularity was defined as the observation of air inside the subepithelial layer with ulceration in the mucosa.

RESULTS

Patient characteristics

A total of 17 patients were selected as the study population (12 men and five women; mean age ± standard

deviation, 46.5 ± 17.1 years; range, 15–70 years). All patients underwent serological ANCA testing (three were MPO-positive, 13 were PR3-positive, and one case was not detected). The patient who did not have a positive ANCA test showed a compatible clinical phenotype confirmed by tissue biopsy and was therefore included in the present study as ANCA-negative GPA. Among the three patients with MPO-positive results, two patients satisfied the GPA criteria while one patient satisfied the MPA criteria (case number 17). The other patients with PR3-positive results satisfied the GPA criteria. The baseline patient characteristics are shown in Table 1.

Imaging features

The imaging findings of patients are indicated in Table 1. AAV showed infiltrative lesions at various sites. The majority of cases showed PNS (88%, 15/17), nasopharynx (88%, 15/17), pterygopalatine fossa (82%, 14/17), and parapharyngeal space (82%, 14/17) involvement. Central skull base involvement was shown by 53% (9/17) of the patients, intracranial involvement by 41% (7/17), and temporal bone involvement by 38% (6/16; Figs 1 and 2, Electronic Supplementary Material Fig. S1). All patients with intracranial involvement had central skull base or temporal bone involvement and most cases (6/7) of intracranial involvement showed dural thickening adjacent to the skull base lesion. Among the patients with temporal bone involvement, five cases showed membranous labyrinth involvement on MRI (Fig 1). Three of five patients with membranous labyrinth involvement showed diffuse enhancement, while the others showed focal nodular enhancement. The involved sites included the vestibule for all patients (5/5), cochlear for 60% (3/5), and semi-circular canal for 40% (2/5). Four of five patients showed bilateral membranous labyrinth involvement, while one showed unilateral involvement. Involvement of the orbit, prevertebral space, and masticator space were seen in 59% (10/17), 47% (8/17), and 18% (3/17) of patients, respectively.

CT revealed bone destruction in 65% (11/17) and bone sclerosis in 71% (12/17) of patients (Figs 1 and 2, Electronic Supplementary Material Fig. S1). In MRI, 67% (10/15) of the patients showed bone marrow signal changes (nine cases with iso-intensity and one case with low signal intensity on T1WI). Soft-tissue necrosis was observed at MRI in 40% (6/15, Fig 1) of the patients, in the nasal cavity, nasopharynx, parapharyngeal space, and masticator space. All lesions (15/15) showed predominant signal iso-intensity to grey matter on T1WI and T2WI. Changes in the mucosa of the PNS and nasopharynx was frequently accompanied by mucosal irregularity (71%, 12/17; Fig 1).

Discussion

The present study reports the CT and MRI findings of AAV involving the skull base. The present series showed that cases of AAV involving the skull base included a wide range of lesions that mostly involved the PNS, nasopharynx,

Table 1
Demographic and imaging features of patients with anti-neutrophil cytoplasmic antibody (ANCA)–associated vasculitis.

No	Sex	Age	Biopsy site	ANCA	Extent								Bone changes		Other MRI findings		
					Paranasal sinuses	Parapharyngeal space	Prevertebral space	Orbit	Pterygopalatine fossa	Central skull base	Temporal bone	Cranial cavity	Destruction	Sclerosis	Signal intensity on T2WI	Signal intensity on T1WI	Soft tissue necrosis
1	F	59	Nasal cavity	PR3	+	+	+	-	+	+	+	+	+	+	Iso to high	Iso	+
2	M	56	Nasal cavity	Not detected	+	+	+	+	+	-	+	+	-	-	Iso to high	Iso	+
3	M	35	Lung	PR3	+	+	+	-	+	-	+	+	+	-	Iso to high	Iso	+
4	M	15	Nasal cavity	PR3	+	+	+	+	+	+	-	+	+	+	Iso to high	Iso	-
5	M	49	Kidney	PR3	+	+	+	+	+	+	+	-	+	+	Iso to high	Iso	+
6	M	40	Left foot dorsum	PR3	+	+	+	+	+	+	+	-	+	+	Iso to high	Iso	-
7	M	52	Nasal cavity	PR3	+	+	-	+	+	+	-	-	+	+	Iso to high	Iso	-
8	M	70	Nasal cavity	PR3	+	+	-	-	+	+	-	-	+	+	Iso to high	Iso	-
9	M	38	Kidney	PR3	+	+	-	+	+	-	-	-	+	+	NA	NA	NA
10	M	58	Lung	PR3	+	+	-	-	+	-	-	-	-	-	Iso to high	Iso	-
11	M	15	Nasal cavity	MPO	+	-	-	-	-	-	-	-	+	+	Iso to high	Iso	+
12	M	22	Nasal cavity	PR3	+	-	-	-	-	-	-	-	+	+	Iso to high	Iso	+
13	F	26	Nasal cavity	PR3	+	+	-	-	+	-	-	-	+	+	NA	NA	NA
14	F	62	Lung	PR3	+	+	+	+	-	+	NA	+	-	+	Iso	Iso	-
15	F	52	Dura	MPO	+	+	-	-	-	-	+	+	+	-	Iso	Iso	-
16	F	38	Kidney	PR3	-	+	+	-	+	-	-	-	-	-	Iso	Iso	-
17	M	61	Kidney	MPO	+	+	-	+	-	+	-	-	-	-	Iso	Iso	-

MRI, magnetic resonance imaging; ANCA, anti-neutrophil cytoplasmic antibody; PR3, predominantly associated with proteinase-3; MPO, myeloperoxidase; T2WI, T2-weighted imaging; T1WI, T1-weighted imaging.
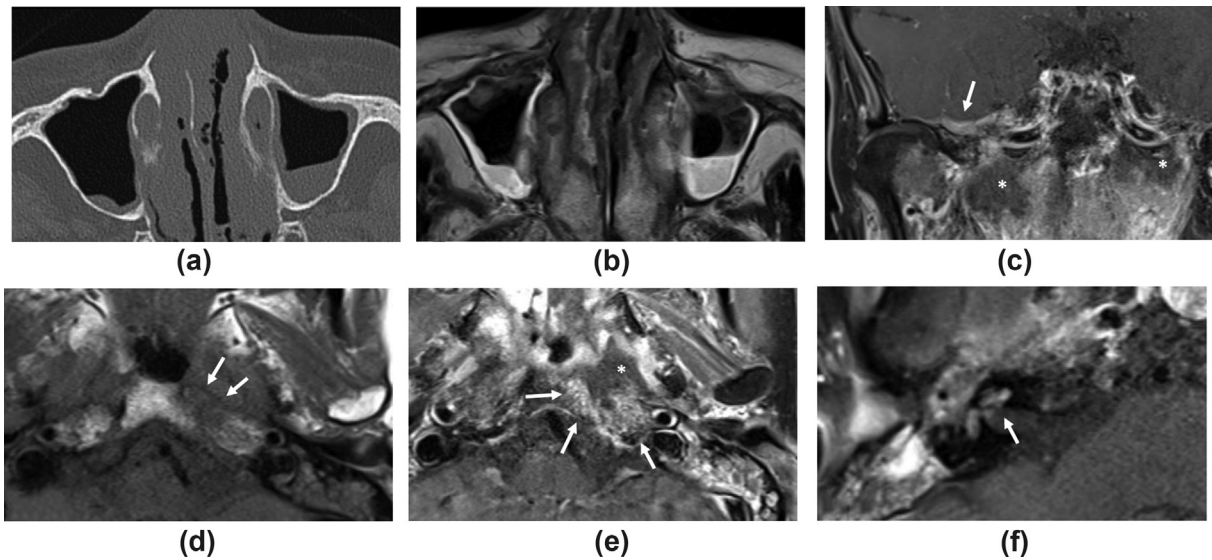
Figure 1 A 38-year-old woman with PR3-positive AVV. (a) Unenhanced CT image showing the mucosal irregularity in both nasal cavities. (b) The involved mucosa shows iso-to low signal intensity on the axial T2WI image. (c) Contrast-enhanced fat-suppressed coronal T1-weighted image shows adjacent dural thickening at the right side (arrows) and a non-enhancing necrotic portion in the parapharyngeal space (asterisk). (d) Axial T1-weighted and (e) contrast-enhanced fat suppressed T1-weighted images show perilesional bone marrow signal change (arrows) in clivus and petrous apex around the soft-tissue necrosis (asterisk). (f) Contrast-enhanced fat-suppressed axial T1-weighted image shows enhancement along cochlear and vestibule, suggesting AVV involvement of the membranous labyrinth.
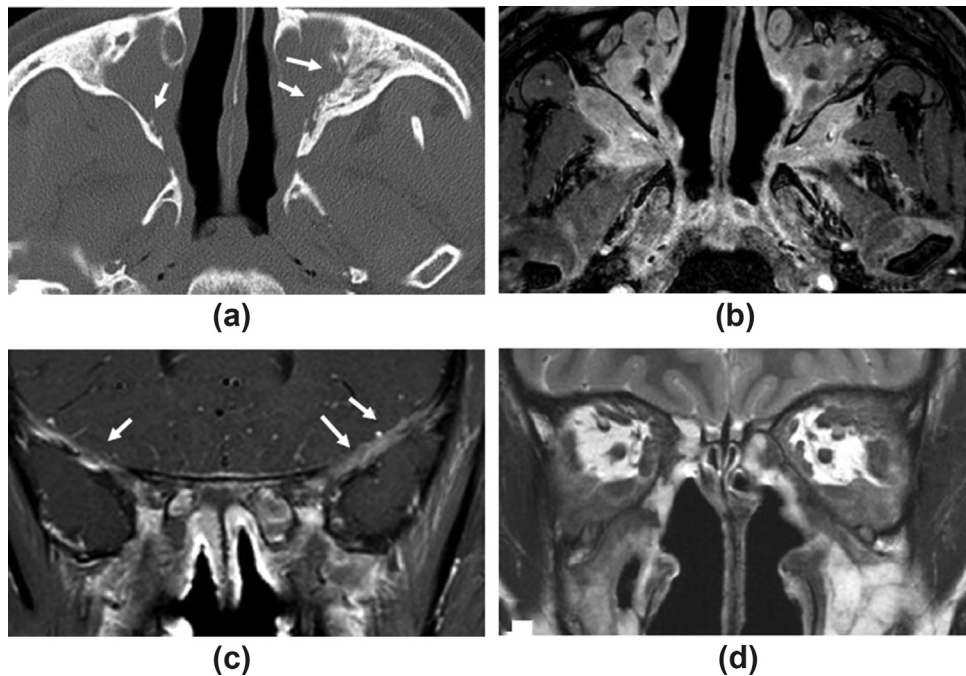
Figure 2 A 15-year-old woman with PR3-positive AVV. (a) Unenhanced CT axial image shows sclerotic changes of the bone (arrows). (b) Contrast-enhanced fat-suppressed axial T1-weighted image shows infiltrating soft-tissue lesion involving both PNS, parapharyngeal space, prevertebral space, orbit, pterygopalatine fossa, and masticator space. (c) Contrast-enhanced fat-suppressed coronal T1-weighted image shows adjacent dural thickening at bilateral side with more severe feature on left side (arrows). (d) Coronal T2-weighted shows involvement of orbit at extraconal and intraconal space.

pterygopalatine fossa, and parapharyngeal space, and were frequently accompanied by mucosal irregularity of the PNS and nasopharynx. Central skull base and temporal bone involvement were seen in 53% (9/17) and 38% (6/16) of patients, respectively.

It is well known that skull base involvement in GPA commonly results from direct extension of the neighbouring granulomatous sinonasal or orbital lesions.[8] Lee *et al.*[13] observed that the lesions in skull base involvement in GPA AAVs were mostly located in the parapharyngeal space

which could also involve the Eustachian tube. Similar to these previous studies, involvement of the PNS and parapharyngeal space was observed in the majority of cases in the present study. The other forms of AAV, MPA and EGPA, rarely involve the skull base.[18,32] In the present study, only one case was classified as MPA, but showed no involvement of the PNS, nasopharynx, or parapharyngeal space.

Sinonasal involvement of the AAV can cause serous otitis media by obstruction of the Eustachian tube.[8] The inner ear structure may be involved by AAV if granulation of the middle ear cavity spreads to the inner ear.[33] Previous studies[34,35] have described the radiological features of the involved inner ear as enhancing lesions in four cases, except for one case, which was examined without contrast media. Similar to these results, the present study showed 33% of patients with AAV had enhancement of the membranous labyrinth on MRI, suggesting destruction of the blood—labyrinthine barrier in the inner ear.

A previous study has reported that the imaging features of the sinonasal involvement of AAV, in particular in GPA, included bone destruction, sclerosis, and mucosal thickening.[8] Benoudiba *et al.* demonstrated that nodular thickening of PNS mucosa on the CT was seen in the patient with GPA.[19] Similarly, in the present study, 71% of patients with AAV showed mucosal irregularity on MRI. The histopathological features of AAV include necrosis and inflammation of the small vessels, and is sometimes associated with thrombosis.[36] In GPA, granulomatous inflammation and areas of necrosis are often confluent, with a "geographic" appearance at low magnification.[1] The "geographic" appearance including microscopic necrosis could be seen as mucosal irregularity on MRI.

Skull base osteomyelitis (SBO) is a potential differential diagnosis for AAV. Key areas for typical SBO include the bony external auditory canal, mastoid tip, temporomandibular joint, petrous apex, petro-occipital fissure, foramen lacerum, jugular foramen, and clivus. From a pathophysiological perspective, typical SBO would appear asymmetrical. Lee *et al.* demonstrated that GPA more frequently showed a parapharyngeal epicentre, homogeneous contrast enhancement, and the absence of necrosis compared with SBO.[13] The frequent incidence of a parapharyngeal epicentre, as observed by Lee *et al.*, is similar to the present findings (the incidence of parapharyngeal involvement in this study was 82% [14/17]), whereas the incidence of necrosis differs. In the present study, necrosis was commonly observed at MRI in AAV (40%). This difference may have occurred because the present study used histopathological confirmation as the reference standard, which can cause selective bias.

The differential diagnosis of AAV includes nasopharyngeal tumours, such as nasopharyngeal carcinoma and nasopharyngeal lymphoma. The important MRI findings to differentiate AAV from nasopharyngeal carcinoma were a parapharyngeal epicentre, a poorly defined margin, and dural involvement.[13] Nasopharyngeal non-Hodgkin's lymphoma (NPNHL) can also involve the skull base, but they more often spread along the pharynx into the nasal cavity or tonsils, rather than extending into the parapharyngeal space or infiltrating superiorly into the skull base.[37,38] The typical imaging feature of NPNHL is a symmetrical and diffuse exophytic tumour that can extend into nasopharyngeal airway without obvious central necrosis, which differs from the findings of AAV[37—39]; however, nasopharyngeal T-cell or natural killer/T-cell non-Hodgkin's lymphomas show a higher incidence of invasion of the nasal cavity and PNS than B-cell lymphomas, which is a finding more similar to AAV.[39] Although rare, Rosai—Dorfman disease can also involve the skull base.[40] Both Rosia—Dorfman disease and AAV involve the dura, but the most common radiological finding in intracranial Rosai—Dorfman disease is an enhancing dural-based mass, which differs from the infiltrative features of AAV.[40,41]

Limitations of the present study include its small sample size and retrospective nature, which may introduce selection bias due to the rarity of this condition. Patients with confirmed skull base involvement were included in the study and selection bias due to this was unavoidable. Patients were enrolled from a tertiary referral hospital over a decade, which indicates the rarity of the presentation, which is a limitation to the power of the study. Second, the study was designed to investigate AAV involving the skull base, but the majority of cases were GPA and only one case of MPA was included in the study. In AAVs other than GPA, head and neck involvement is rare. In particular, according to the MPA criteria, if there is bloody nasal discharge, ulcers, crusting, congestion, or blockage, and septal defect/perforation, the diagnostic possibility is decreased (score: −3),[28] which makes it difficult to find patients who are diagnosed as MPA with head and neck involvement.

In conclusion, the present case series revealed that an image finding of AAV involving the skull base mostly appears as an infiltrative lesion predominantly involving the PNS, nasopharynx, pterygopalatine fossa, and parapharyngeal space. It is frequently accompanied by mucosal irregularity and bone change. The presence of soft-tissue necrosis or membranous labyrinth involvement was not rare. Although the radiological findings are non-specific and skull base involvement of AAV is less common, identifying the imaging finding of AAV with skull base involvement and correlation with laboratory results and clinical features can be helpful for diagnosis of AAV.

Conflict of interest

The authors declare no conflict of interest.

Appendix A. Supplementary data

Supplementary data to this article can be found online at https://doi.org/10.1016/j.crad.2023.04.004.

References

1. Kitching AR, Anders H-J, Basu N, *et al.* ANCA-associated vasculitis. *Nat Rev Dis Primers* 2020;**6**(1):1—27.
2. Jennette JC, Falk R, Bacon P, *et al.* Revised international Chapel Hill consensus conference nomenclature of vasculitides. *Arthritis Rheum* 2012;**65**(1):1—11.

3. Falk RJ, Gross WL, Guillevin L, *et al*. Granulomatosis with polyangiitis (Wegener's): an alternative name for Wegener's granulomatosis. *Ann Rheum Dis* 2011;**70**(4):704.

4. Berti A, Cornec D, Crowson CS, *et al*. The epidemiology of antineutrophil cytoplasmic autoantibody—associated vasculitis in Olmsted County, Minnesota: a twenty-year US population-based study. *Arthritis Rheum* 2017;**69**(12):2338—50.

5. Mohammad A, Jacobsson L, Mahr A, *et al*. Prevalence of Wegener's granulomatosis, microscopic polyangiitis, polyarteritis nodosa and Churg—Strauss syndrome within a defined population in southern Sweden. *Rheumatology* 2007;**46**(8):1329—37.

6. Jennette JC, Falk RJ. Small-vessel vasculitis. *N Engl J Med* 1997;**337**(21):1512—23.

7. Greco A, Marinelli C, Fusconi M, *et al*. Clinic manifestations in granulomatosis with polyangiitis. *Int J Immunopathol Pharmacol* 2016;**29**(2):151—9.

8. Pakalniskis MG, Berg AD, Policeni BA, *et al*. The many faces of granulomatosis with polyangiitis: a review of the head and neck imaging manifestations. *AJR Am J Roentgenol* 2015;**205**(6):W619—29.

9. Carpentier A, Riehm S, Charpiot A, *et al*. Wegener's granulomatosis of the temporal bone and skull base that mimicked an inflammatory myofibroblastic tumour: a case report. *B-ENT*. 2010;**6**(2):135—8.

10. Qureshi HA, Bandhlish A, DeConde RP, *et al*. Initial presentation of granulomatosis with polyangiitis as progressive skull base osteomyelitis. *ORL J Otorhinolaryngol Relat Spec* 2022;**84**(4):342—6.

11. Lotfallah A, Shahidi S, Odelberg SW, *et al*. Seronegative granulomatosis with polyangiitis presenting as an acute skull base osteomyelitis with multiple cranial neuropathies. *J Surg Case Rep* 2021;**2021**(10):rjab476.

12. Maramattom BV, Thomas J, Nair S. Antineutrophil cytoplasmic antibody vasculitis causing skull base inflammation and aortitis. *Ann Indian Acad Neurol* 2018;**21**(4):339.

13. Lee B, Bae YJ, Choi BS, *et al*. Radiologic differentiation between granulomatosis with polyangiitis and its mimics involving the skull base in humans using high-resolution magnetic resonance imaging. *Diagnostics* 2021;**11**(11):2162.

14. Andrews JT, Kountakis SE. Wegener's granulomatosis of the skull base. *Am J Otolaryngol* 1996;**17**(5):349—52.

15. Bernat AL, Lefevre E, Sene D, *et al*. Management scheme for cerebral Wegener granulomatosis: an unusual pseudotumoral skull base pathology. *World Neurosurg* 2016;**96**:608. e613—e608. e616.

16. Sharma A, Deshmukh S, Shaikh A, *et al*. Wegener's granulomatosis mimicking skull base osteomyelitis. *J Laryngol Otol* 2012;**126**(2):203—6.

17. Harrison L, Mcnally J, Corbridge R. Granulomatosis with polyangiitis affecting the skull base and manifesting as spontaneous skull base osteomyelitis. *Case Rep* 2016;**2016**:bcr2015213912.

18. Kim S-H, Park J, Bae JH, *et al*. ANCA-negative Wegener's granulomatosis with multiple lower cranial nerve palsies. *J Korean Med Sci* 2013;**28**(11):1690—6.

19. Benoudiba F, Marsot-Dupuch K, Rabia HM, *et al*. Sinonasal Wegener's granulomatosis: CT characteristics. *Neuroradiology* 2003;**45**(2):95—9.

20. Lohrmann C, Uhl M, Warnatz K, *et al*. Sinonasal computed tomography in patients with Wegener's granulomatosis. *J Comput Assist Tomogr* 2006;**30**(1):122—5.

21. Cleary JO, Sivarasan N, Burd C, *et al*. Head and neck manifestations of granulomatosis with polyangiitis. *Br J Radiol* 2021;**94**(1119):20200914.

22. Kato K, Sone M, Teranishi M, *et al*. Inner ear 3D-FLAIR magnetic resonance image evaluation of MPO-ANCA related angitis patients. *Nihon Jibiinkoka Gakkai Kaiho* 2013;**116**(11):1192—9.

23. Kawashima Y, Noguchi Y, Ito T, *et al*. Otologic manifestations in patients with ANCA associated vasculitis-comparative analysis among microscopic polyangiitis, granulomatosis with polyangiitis and eosinophilic granulomatosis with polyangiitis. *Nihon Jibiinkoka Gakkai Kaiho* 2016;**119**(2):110—7.

24. Thajeb P, Tsai JJ. Cerebral and oculorhinal manifestations of a limited form of Wegener's granulomatosis with c-ANCA—associated vasculitis. *J Neuroimaging* 2001;**11**(1):59—62.

25. Vandenbroucke JP, von Elm E, Altman DG, *et al*. Strengthening the reporting of observational studies in epidemiology (STROBE): explanation and elaboration. *Ann Intern Med* 2007;**147**(8):W163—94.

26. von Elm E, Altman DG, Egger M, *et al*. The Strengthening the Reporting of Observational Studies in Epidemiology (STROBE) statement: guidelines for reporting observational studies. *J Clin Epidemiol* 2008;**61**(4):344—9.

27. Salvador F. ANCA associated vasculitis. *Eur J Intern Med* 2020;**74**:18—28.

28. Robson J, Grayson P, Ponte C, *et al*. Classification criteria for the ANCA-associated vasculitides. kez058.050 *Rheumatology* 2019;**58**(Suppl. 2). 110.

29. Borges A. Imaging of the central skull base. *Neuroimaging Clin N Am* 2009;**19**(3):441—68.

30. Conley LM, Phillips CD. Imaging of the central skull base. *Radiol Clin* 2017;**55**(1):53—67.

31. Peters JE, Gupta V, Saeed IT, *et al*. Severe localised granulomatosis with polyangiitis (Wegener's granulomatosis) manifesting with extensive cranial nerve palsies and cranial diabetes insipidus: a case report and literature review. *BMC Neurol* 2018;**18**(1):1—13.

32. Watts RA, Scott DG, Mukhtyar C. Eosinophilic granulomatosis with polyangiitis—EGPA (Churg—Strauss syndrome). In: *Vasculitis in clinical practice*. Cham: Springer; 2015. p. 79—90.

33. Yoshida N, Iino Y. Pathogenesis and diagnosis of otitis media with ANCA-associated vasculitis. *Allergol Int* 2014;**63**(4):523—32.

34. Sone M, Mizuno T, Naganawa S, *et al*. Imaging analysis in cases with inflammation-induced sensorineural hearing loss. *Acta Otolaryngol* 2009;**129**(3):239—43.

35. Watanabe T, Yoshida H, Kishibe K, *et al*. Cochlear implantation in patients with bilateral deafness caused by otitis media with ANCA-associated vasculitis (OMAAV): a report of four cases. *Auris Nasus Larynx* 2018;**45**(5):922—8.

36. Ball GV, Fessler BJ, Bridges SL. *Oxford textbook of vasculitis*. Oxford: Oxford University Press; 2014. p. 101—8.

37. Liu X-w, Xie C-m, Mo Y-x, *et al*. Magnetic resonance imaging features of nasopharyngeal carcinoma and nasopharyngeal non-Hodgkin's lymphoma: are there differences? *Eur J Radiol* 2012;**81**(6):1146—54.

38. King A, Lei K, Richards P, *et al*. Non-Hodgkin's lymphoma of the nasopharynx: CT and MR imaging. *Clin Radiol* 2003;**58**(8):621—5.

39. Xie C-m, Liu X-w, Mo Y-x, *et al*. Primary nasopharyngeal non-Hodgkin's lymphoma: imaging patterns on MR imaging. *Clin Imaging* 2013;**37**(3):458—64.

40. Hollon T, Camelo-Piragua SI, McKean EL, *et al*. Surgical management of skull base Rosai—Dorfman disease. *World Neurosurg* 2016;**87**:661.e5-12.

41. Huang BY, Zong M, Zong WJ, *et al*. Intracranial rosai—dorfman disease. *J Clin Neurosci* 2016;**32**:133—6.